
Final Project Report

Project Title: High Altitude Radiation Detector (GU-HARD-PL03)

Institution: Gannon University

Contact Author: Dr. Wookwon Lee

Dept. of Electrical and Computer Engineering

Gannon University

109 University Square, Erie, PA 16541

Email: lee023@gannon.edu

Project Duration: 01/01/2013 – 12/13/2013

Date submitted: 12/13/2013

Table of Contents

1.	Project Overview.....	4
2.	Payload Subsystems.....	6
2.1.	Detector Module.....	6
2.2.	Comparator Module	8
2.3.	Coincidence Detector.....	8
2.4.	Microprocessor/CPU.....	8
2.5.	Power Module.....	9
3.	Key Revision Aspects.....	10
4.	Numerical Results and Discussions.....	10
4.1.	Lab Testing Data – Detector and Comparator Modules	10
4.2.	In-Flight Experimental Data	12
5.	Lessons Learned.....	16
6.	Participants	17
7.	Presentations and Publications.....	18
8.	Reflections and Implications	18
9.	Concluding Remarks.....	18
	References	20
	Appendix	21
A-1.	Software Subroutines for Micro-processor	21

List of Figures

Figure 1. Overall functional block diagram for the HASP2013 HARD payload	4
Figure 2. Setup for lab testing.....	5
Figure 3. Completed, sealed GU-HARD-PL03.....	5
Figure 4. Exploded view of the 2012 payload	6
Figure 5. Detector module, including scintillator, rotator and e-compass.....	6
Figure 6. Detector module: (a) photo diode and scintillator (b) integration with a preamplifier	6
Figure 7. Application circuit diagram of the pre-amplifier for SiPM [3]	7
Figure 8. Fully assembled detector module with the rotator module.....	7
Figure 9. Power system diagram.....	9
Figure 10. Voltage divider chain to provide HASP 2013 SiPM bias voltage	11
Figure 11. Output signals: (a) SiPM amplifier (b) OP AMP (comparator)	12
Figure 12. (a) Internal payload temperature during flight, (b) e-compass heading	13
Figure 13. Event rates	14

List of Tables

Table 1. Testing Data of the Detector Module	10
----------------------------------------------------	----

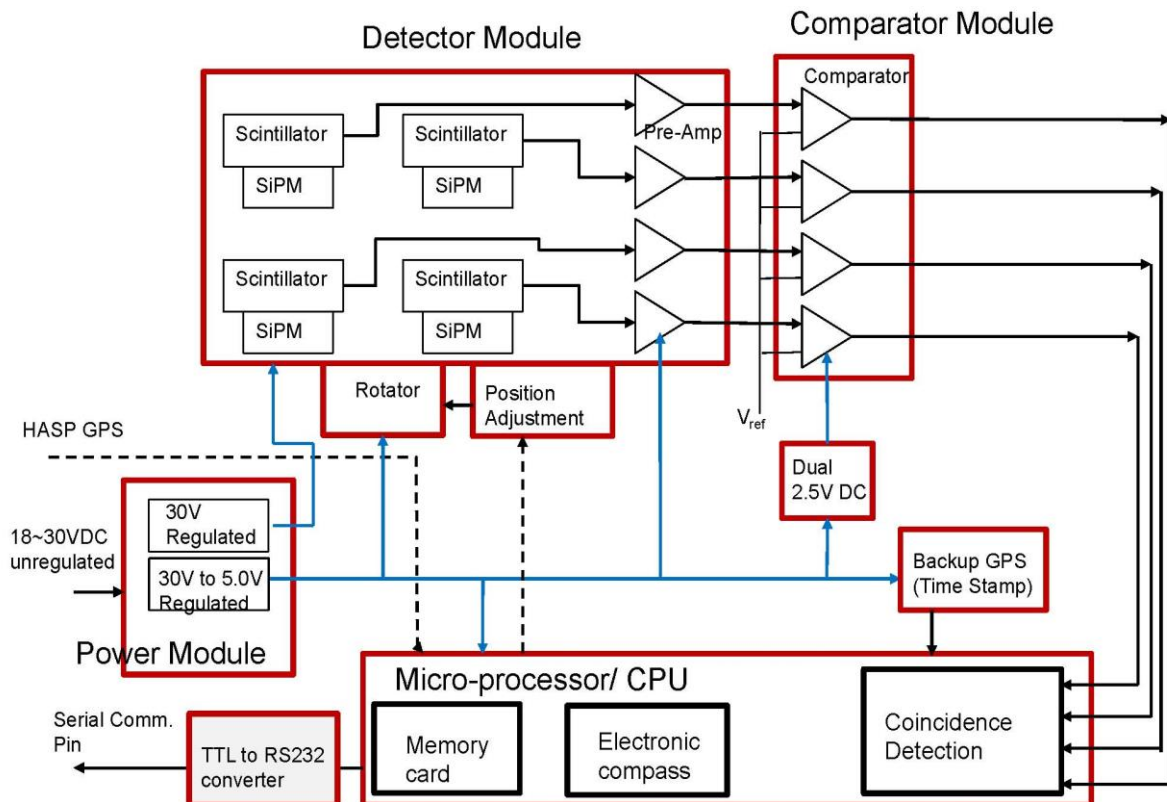
Definition of Acronyms

Acronyms	Definition
CPU	Central Processing Unit
CSBF	Columbia Scientific Balloon Facility
FLOP	Flight Operation Plan
HARD	High Altitude Radiation Detector
OP AMP	operational amplifier
PMT	Photomultiplier Tube
PSIP	Payload Specification & Integration Plan
SiPM	Silicon Photomultiplier

1. Project Overview

Science Objectives – Gannon University’s High Altitude Radiation Detection (HARD) payload #3, GU-HARD-PL03, is a redesign of HARD payload #2, GU-HARD-PL02, which Gannon University designed, built, and flew for the HASP2012 flight. The payload PL02 had several problems during flight that prevented it from collecting the desired science data. The payload constructed for the HASP 2013 flight is entirely new (not a modification of the previous one) and intended to fix the problems encountered previously.

The primary project objective is, very similar to that for PL02, to investigate how the “east-west” angular asymmetry changes with altitude, as the cosmic ray flux transitions from mostly secondary particles near ground level to mostly primary cosmic rays near balloon-float altitudes [1]. This asymmetry exists because the Earth’s magnetic field deflects cosmic-ray trajectories from a straight line. Since cosmic rays are predominantly positively charged, more cosmic rays arrive from the west than from the east. This asymmetry has been investigated in the past on the ground, in planes, and even with balloons. Additionally, this project intends to study how the intensity of cosmic rays changes with altitude, based on measurements of cosmic ray intensity from multiple arrival directions, providing a more complete picture of the high-altitude radiation environment caused by cosmic rays.



Payload Subsystems – The overall design of the payload is very similar to last year, although lessons learned from the previous flight have been incorporated into the design (such as including a TTL to RS232 converter for serial communications). The payload has been designed using a top-down approach: engineering requirements were established, followed by functional decomposition, and finally design and construction of subsystems by the student team from the Electrical and Computer Engineering department. The functional block diagram of the payload is shown in Figure 1, and the subsystems will be described in more detail in the following section. The completed payload, prior to integration and thermal vacuum test at the Columbia Scientific Balloon Facility (CSBF) lab, is shown in Figure 2.

Project Milestones and Deliverables – The team delivered monthly status reports on project progress from January 2013 to November 2013, a Payload Specification & Integration Plan (PSIP), Flight Operation Plan (FOP), and on-site payload integration at the CSBF lab.

Participants – The student team consisted of a total of six ECE undergraduate students, including one senior and five juniors (as of Sept. 2013), and two faculty advisors from the ECE and Physics departments.



Figure 2. Completed, sealed GU-HARD-PL03

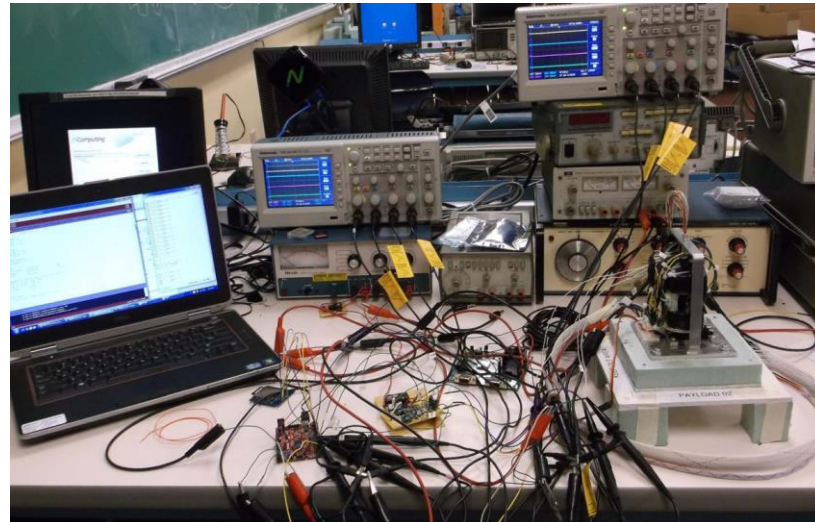


Figure 3. Setup for lab testing

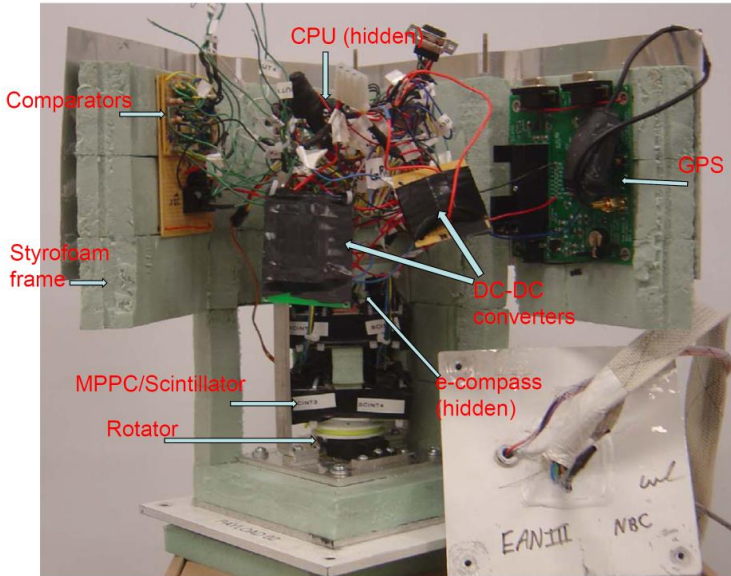


Figure 4. Exploded view of the 2012 payload (similar to the 2013 payload, GU-HARD-PL03)

2. Payload Subsystems

As with the 2012 payload, the key subsystems are the detector module, comparator module, coincidence detector, microprocessor/central processing unit (CPU), and power module. A brief description of each module is given below. A photo of the payload in the lab prior to integration is shown in Figure 3, and an exploded view of the 2012 payload after flight is shown in Figure 4. While the 2013 payload differed slightly in the placement of modules on the sides of the support structure, the layout was very similar.

2.1. Detector Module

In order to detect cosmic rays in the east-west plane, an array of four active detector elements is arranged in a square, as shown in Figure 5. Each active detector element consists of a Photonique SiPM 0905V13MM silicon photomultiplier (SiPM) [2] attached via optical epoxy to a $3 \times 3 \times 1 \text{ cm}^3 \text{CsI(Tl)}$ scintillating crystal, as shown in Figure 6(a). The scintillating crystals emit light when traversed by a charged particle, which

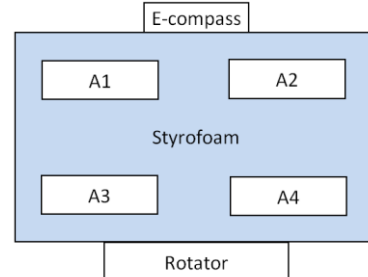


Figure 5. Detector module, including scintillator, rotator and e-compass

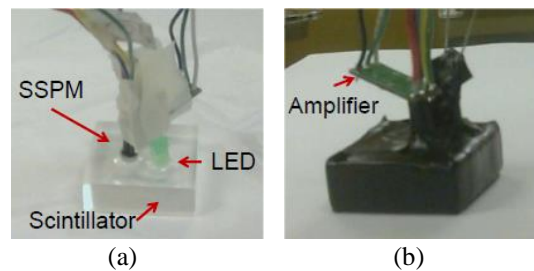


Figure 6. Detector module: (a) photo diode and scintillator (b) integration with a preamplifier

can be detected by the SiPMs and converted into an electric pulse. Green LEDs were also glued to the scintillator to supply light for lab testing purposes. In order to capture as many photons as possible via the SiPM, the entire scintillator is wrapped in white Teflon to reflect stray photons back into the detector. The unit is then covered in black electrical tape to prevent ambient light from entering the detector. A completed scintillator is shown in Figure 6(b).

SiPMs were selected over traditional photomultiplier tubes (PMTs) for this payload due to their low bias voltage (~ 30 V). Most PMTs require an operating voltage of ~ 1 kV. In the near vacuum encountered at balloon float altitudes, high voltages must be carefully potted to avoid dielectric breakdown, a shortcoming not shared by SiPMs. They are also very compact, less expensive, and consume less power.

Each SiPM unit outputs a voltage proportional to the number of detected photons. However, this voltage signal is small and negative. As such, a pre-amplifier is also connected to each SiPM, which generates a negative pulse ranging from 0 to around -1 V, depending on the amount of light generated within the scintillator. The application circuit of the pre-amplifier used for the detector module is shown in Figure 7 where capacitors C1 and C2 have a typical value of 10 nF.

Due to the long scintillation decay time of CsI(Tl) crystals, the output pulses from the pre-amplifier were typically ~ 1 μ s in duration (although the rise-time of the pre-amp was much faster, around 5 ns). Manipulation and detection of these short pulses required fast electronics, which drove many design decisions for the comparator and coincidence detector.

The detector array must maintain an orientation in the east-west plane to detect the east-west asymmetry. An HMC6352 electronic compass [4] is used to determine the orientation of the detector module. When the orientation of the payload drifts more than 10° from the desired orientation due to rotation of the HASP platform, a servo motor is used to adjust the detector. The completed detector module, including the e-compass and rotator is shown in Figure 8.

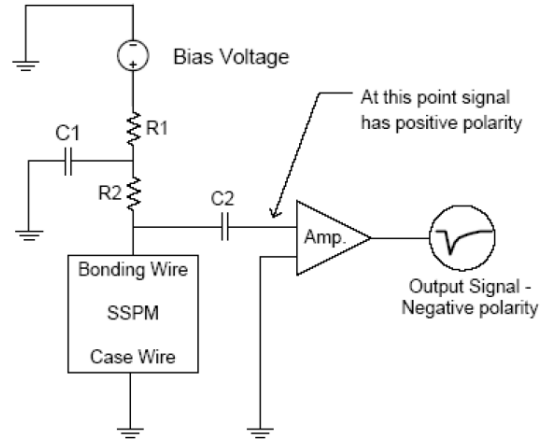


Figure 7. Application circuit diagram of the pre-amplifier for SiPM [3]

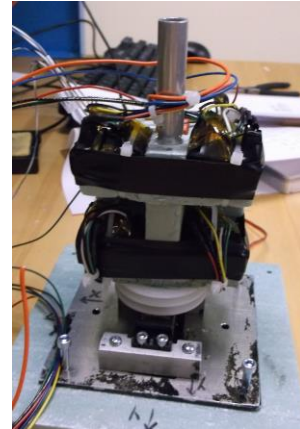


Figure 8. Fully assembled detector module with the rotator module

The failure mode seen in last years payload (continuous triggering even without a valid signal) was observed during bench testing of the detector module this year. This condition was encountered while the servo motor was drawing current. The servo was controlled using pulse width modulation, meaning that the angle of the servo was controlled by sending a pulse whose width defined the angle of rotation. The flight code resent this control pulse every 20 ms, even when the servo was in position, which sometimes caused the servo to attempt to slightly adjust its rotation. The anomalous trigger rate problem was solved by only sending the control pulse when the servo needed adjustment.

2.2. Comparator Module

The Comparator Module consists of four comparators. The function of each comparator is to convert the analog output signal from the SiPM amplifier into a digital signal to be used as an input for the coincidence detector. Since the SiPM amplifier outputs a negative voltage, an inverting comparator circuit was constructed using an AD8616 [5] inverting operational amplifier (OP AMP) with a high voltage gain to produce a TTL logic-level signal (e.g., smaller or greater than a amplitude threshold of about +2.4 V) for the microprocessor. From experience with the previous payload, the team realized that a traditional LM741 OP AMP did not have sufficient gain at high frequencies.

2.3. Coincidence Detector

The Coincident Detector is implemented as one of several subroutines within the microprocessor/CPU. The four outputs from the Comparator Module are connected to digital input pins of the microcontroller. To monitor for a simultaneous coincidence in two or more SiPM modules, the microcontroller polls the digital input pins approximately once a microsecond to obtain a Boolean value, which will be logical “0” if the SiPM has no output and “1” if the SiPM outputs a signal. The microcontroller then looks for the coincidence of two or more of the SiPMs simultaneously returning a logical value of 1. When this condition is met, the microcontroller recognizes it as a successful “hit” (i.e., an event).

2.4. Microprocessor/CPU

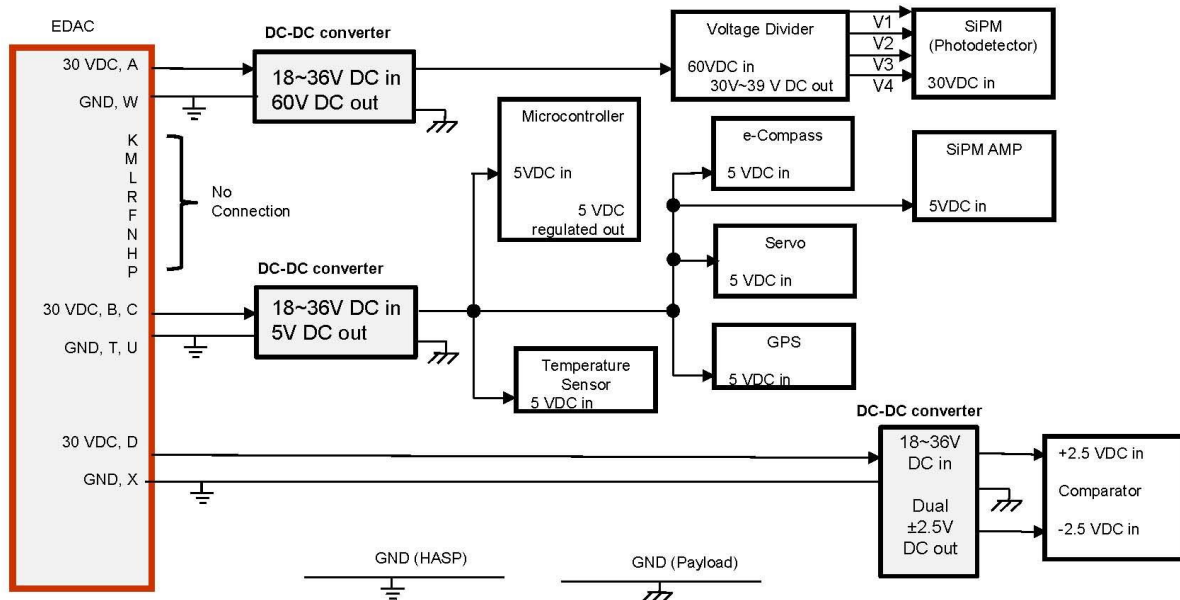
A chipKIT Uno32 Prototyping Platform [6] is used as the main microprocessor module. In addition to polling the digital I/O pins to determine whether a coincidence condition has been met, as described above, the microprocessor provides a number of other functions. These include facilitating serial communication with HASP, collecting data from a temperature sensor attached to the 60 V power supply, controlling the servo to adjust detector orientation, and collecting GPS time. As was learned from the previous flight, the serial port on the Uno32 works with TTL logic voltage levels (0 ~3.3 V), whereas the HASP equipment requires RS-232 logic levels (-15 ~ 15 V). Therefore, a MAX233 line driver/receiver [7] is used to convert the TTL logic of the microprocessor to RS-232 logic as required to enable serial communication with HASP.

The programming codes were implemented in Arduino via the chipKIT provided MPIDE (see Appendix for a list of subroutines). All code was thoroughly tested in the lab prior to the flight. The original design called for the microcontroller to write individual events to an SD card during flight, but the MPIDE SD

library code was not stable and occasionally caused the payload to lock up. Rather than risk such a lockup during flight, the SD card was disabled, and the team relied solely on data transmitted via serial to HASP.

2.5. Power Module

The HASP system provides an unregulated 30 V power supply, which was converted into the regulated voltages required by the payload by using DC-DC converters. A Murata NDY2405C isolated DC-DC converter [8] is used to supply 5V power to the microprocessor, GPS, temperature sensor, TTL to RS232 converter, servo, and the e-compass. Since the comparator requires a ± 2.5 V power supply, the same Murata 5 V supply was used, in conjunction with a voltage divider grounded between the resistors of the divider chain, to provide this voltage. Use of an isolated power supply allows the payload ground to differ from the HASP ground. Since each SiPM requires a different voltage in the range of 30 ~ 40V, two RS-2415D/H2 [9] are used in series to obtain 60V and then a voltage divider circuit is used to provide 34 ~ 38V to the SiPMs. This SiPM supply voltages were selected based on test conditions described in Section 4.1. Figure 9 shows the payload power system diagram.



- [Notes]
- GND (HASP) and GND (Payload) are not to be connected as they are separated by the isolated DC-DC converters.
 - All ground pins of the subsystems of the payload shall be connected to GND (Payload).
 - The common ground of the dual power supply (for the Comparator) shall be connected to GND (Payload).

Figure 9. Power system diagram

3. Key Revision Aspects

Revisions to the design of HARD PL03 were based on observations of data from the 2012 flight and also qualitative analysis of failure mode and effect. The following design aspects, which were identified as potential sources of problems from the previous flight, have been improved for the 2013 payload.

SiPM – The precision of the SiPM bias voltage was identified as a potential cause of the false triggering in the 2012 payload. While the source of that error has now been identified as the servo motor, the design of the payload was improved by using a more complex divider chain with variable resistors so that the bias voltage to each SiPM could be adjusted individually.

Power module and rotator – For the 2012 payload, the overall ground level was somewhat unstable, especially when the rotator operated, resulting in a large signal in the SiPM amplifier output. For this payload, much more attention was invested in thinking about the payload ground. This in fact turned out to be the main cause of the failure of the previous payload, although it was not realized at the time that the servo was drawing current even when not rotating. As mentioned above, the undesired behavior was corrected by ensuring that the servo control pulse was only sent while the detector module needed to rotate. This error mode did not reoccur during the 2013 flight.

4. Numerical Results and Discussions

4.1. Lab Testing Data – Detector and Comparator Modules

The performance of the SiPM units depended significantly on the supplied bias voltage, with larger bias voltages giving more gain in the output. Unit testing of SiPMs revealed that only four units and amplifiers were working properly, thus tuning the bias voltage to these units was crucial. In order to allow the bias voltage to each SiPM to be precisely adjusted as necessary, the voltage divider for the HASP 2013 flight was redesigned using variable resistors. The circuit for this divider chain is shown in Figure 10. The LED glued to each scintillator unit was flashed with a pulse whose duration and intensity was similar to a typical muon passing through the scintillator. The bias voltage for each SiPM was adjusted to give an approximately 1 V output from the amplifier for a typical muon event. The results of this test are shown in Table 1. **Table 1** In order to ensure that each detector module had a similar single event trigger rate, the

Table 1. Testing Data of the Detector Module

Detector Module	Test 1	Test 2
	SiPM Bias Voltage [V]	SiPM Bias Voltage [V]
	Test condition: Preamplifier output: at negative peak voltage < -1V	
A1	33.6	33.6
A2	35.9	35.7
A3	35.9	35.9
A4	33.6	33.5

system was run in a mode to count single coincidences from the comparator. The bias voltage was further adjusted so that all modules had single event rates that were similar. As can be seen in Table 1, this required only minor adjustment.

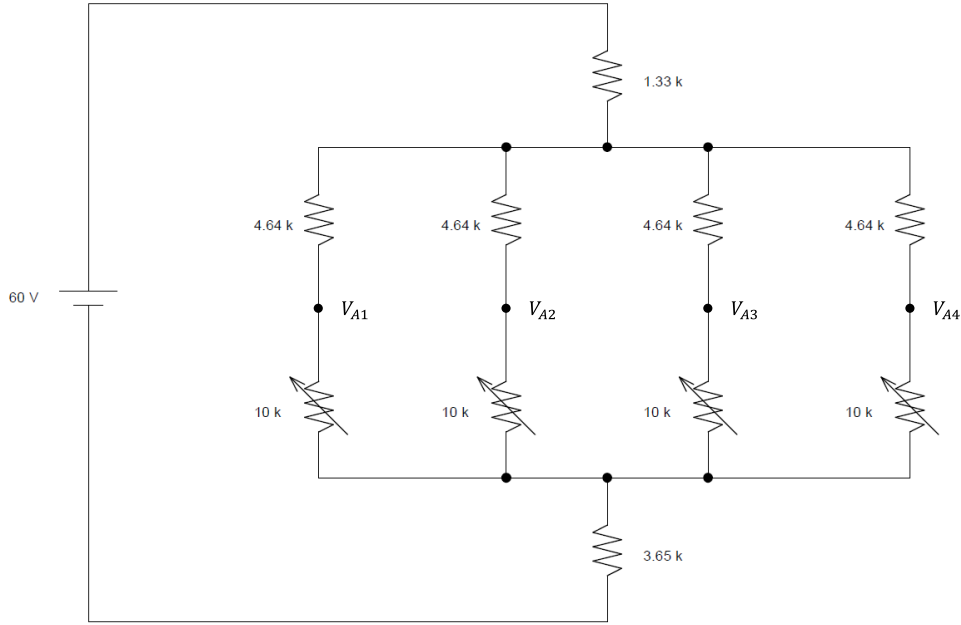


Figure 10. Voltage divider chain to provide HASP 2013 SiPM bias voltage. V_{A1} , V_{A2} , V_{A3} , and V_{A4} are the bias voltages to scintillator modules A1, A2, A3 and A4, respectively.

The output of a SiPM amplifier is illustrated in Figure 11(a) for a muon traversing a completed detector module, while the corresponding comparator output can be seen in Figure 11(b). The negative output from the SiPM amplifier resulted in a positive output pulse from the comparator with similar period, about 1.8 μ s. As discussed previously, the output of the high-gain, high-bandwidth OP amp used for the comparator had an amplitude of ~ 2.5 V, which was sufficient for the logical operation of the micro-controller.

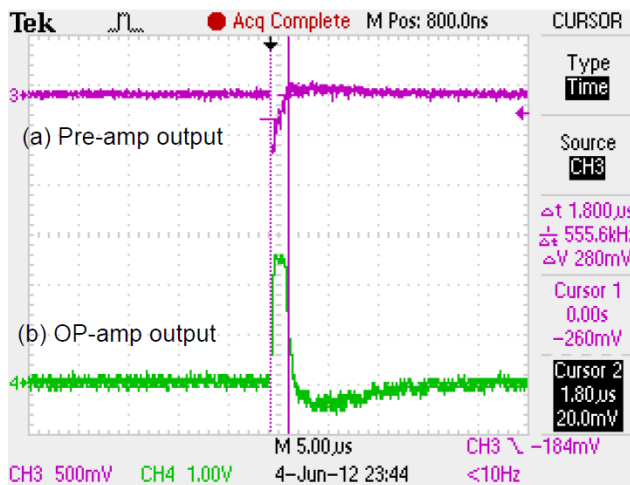


Figure 11. Output signals: (a) SiPM amplifier (b) OP AMP (comparator)

4.2. In-Flight Experimental Data

The HASP 2013 version of our payload was flight-certified after a 2nd attempt to pass the thermal vacuum testing at the CSBF site. The payload launched at 2:57pm UTC on September 2, 2013, and terminated at 4:11 am UTC on September 3, 2013 after ~10.5 hrs at float altitude. Our payload turned on during climb out and transmitted data to the ground via serial communication with HASP for the entire flight duration, although there were some outages due to unknown communication interruptions. Data collected during the flight is presented below.

A temperature sensor was attached to the 60 Vdc power supply to monitor the payload, as this was the component that drew the most power and would therefore have the highest temperature. As shown in Figure 12(a), this temperature ranged from approximately -2°C to 44°C except for one anomalous data point at -50°C. This data point is most likely due to a sensor or transmission error, as cooling and reheating the payload so quickly is extremely unlikely. Otherwise, the payload temperature was well within the safe operating limits of all payload components and actually remained rather consistent throughout the flight.

In order to measure the east-west assymetry, the payload had to maintain an orientation in the east-west plane. An electronic compass monitored the payload orientation and a servo was rotated if the e-compass deviates from due north by more than 10 degrees. From Figure 12(b), it is clear that this system functioned properly during flight, as the e-compass never deviates from northward reading by more than 10 degrees (between the red lines), except for three times when the system was intentionally disabled around 500, 700, and 800 minutes into the flight. During these times, the payload was rotated by 180° with the intention of gathering data pointing due south to better understand systematic errors.

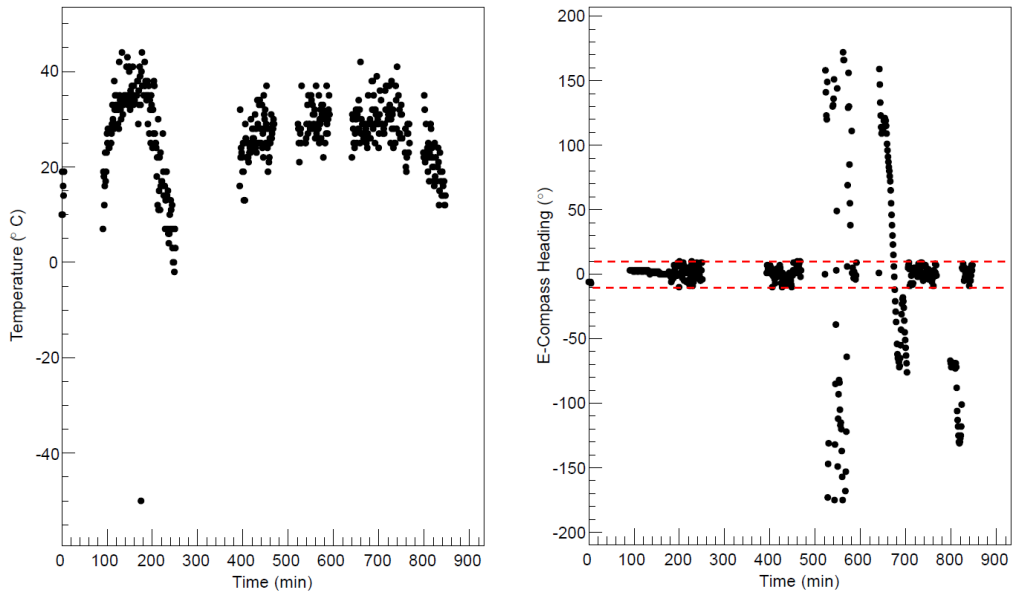


**Figure 12. (a) Internal payload temperature during flight, (b) e-compass heading
(Red lines indicate deviation of 10° from due north).**

During the first period where the autorotation was disabled, the reading from the e-compass changed erratically. It is unlikely that the HASP platform was rotating at the high rate implied by this data. However, significant swaying of the HASP platform could cause this type of erratic reading, which seems entirely reasonable. This does raise some serious question as to the accuracy of the e-compass for periods in the flight preceding this point. Data from the rotation angle of the servo would provide a useful handle for understanding how often the payload was re-oriented (which should be rare). Unfortunately, this data was not recorded and is therefore lost. Recording this data would be advisable for future revisions to this or similar payloads. A three axis electronic compass, perhaps combined with a gyroscope, could probably have provided more accurate heading information despite the swaying.

Data from the second and third periods where the autorotation was disabled resulted in data where the e-compass reading changed smoothly, although the payload seems not to have rotated to exactly 180° at the beginning of either period. This is more consistent with a slower rotation of the HASP platform, although an approximately 3 degree/minute rotation still seems a little high. Unfortunately, data while the instrument was pointing south was not collected, thus understanding systematic errors (such as one detector module being slightly larger or out of position) during flight will be challenging. A dedicated autorotation function for pointing south instead of north could be implemented on a future payload to eliminate this problem.

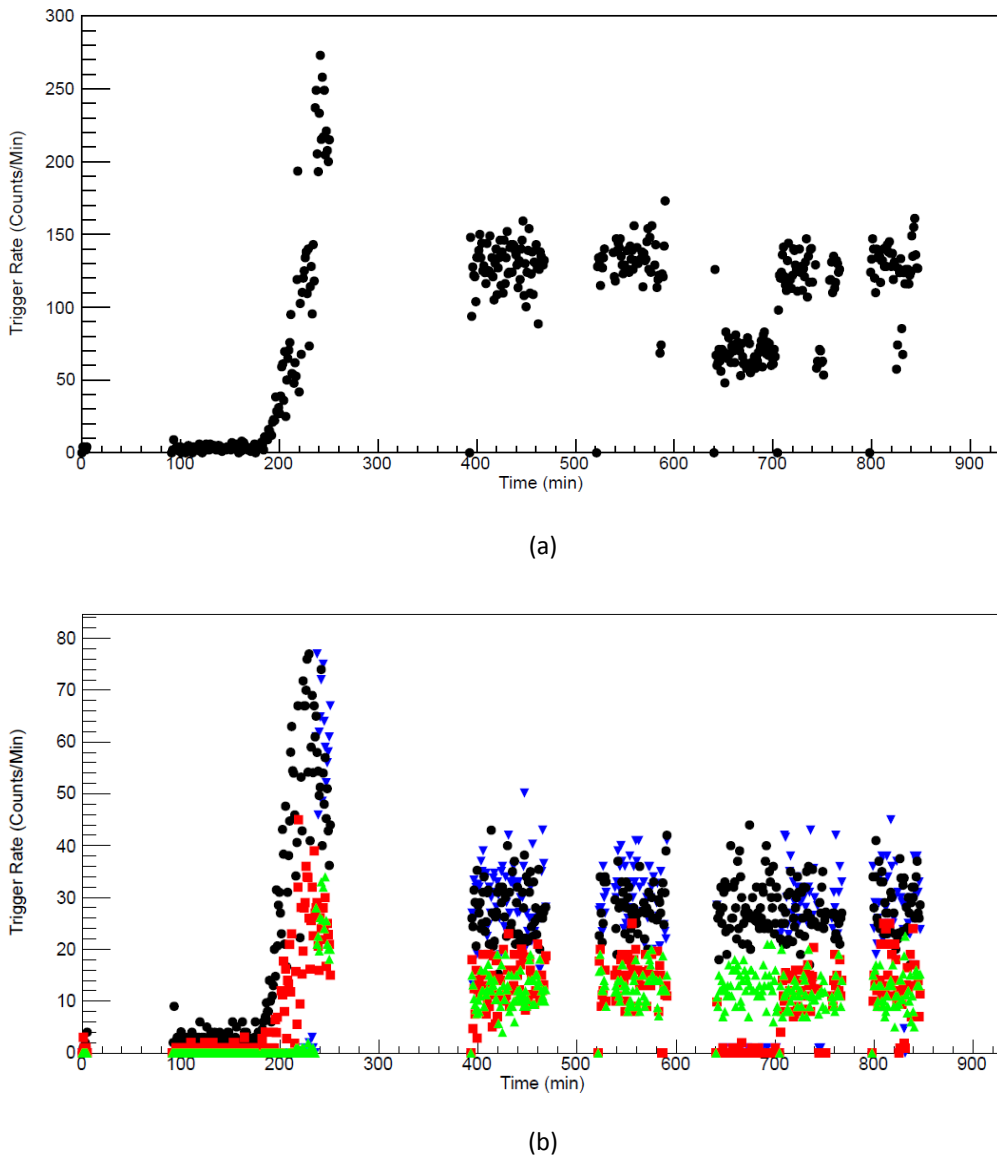


Figure 13. Event rates

(a) Total event rate (in counts per minute) for all directions. **(b)** Event rate for downward events through A1 and A3 (blue downward triangles), downward events through A2 and A4 (black circles), east going events (red squares), and west-going events (green upward triangles)

Figure 13(a) shows the total instrument event rate, which is the number of simultaneous coincidence events per minute. As expected, the rate starts from a few events per minute at ground level and increases rapidly as the balloon ascends. Unfortunately, the instrument stopped transmitting data before reaching a maximum event rate, but it is clear that the rate decreased as HASP reached float altitude. This is consistent with expectations, because muon production from extended air showers results in maximum radiation rate around $\sim 40,000\text{-}50,000$ ft. The instrument trigger rate remained reasonable constant

between 100 and 150 counts/minute for the remainder of the flight, except for around 650 minutes into the flight, where it drops to about half.

To better understand this anomalous drop in total trigger rate, the rates from the different combinations of scintillators are show in Figure 13(b). A number of features stand out in this figure. First, the trigger rate for one of the downward going combinations (detector modules A1 and A3) is has no data for the first few hours of the flight. A similar situation exists for the westward-going events (detector modules A2 and A3). The most obvious conclusion from this observation is that either detector module A3 or the associated comparator channel stopped functioning. Post-analysis of the thermal vacuum data revealed that A3 stopped transmitting data during the second vaccum test. Fortunately, it began functioning again part way through the flight and continued working for most of the remainder of the flight. However, at the time of the total trigger rate drop mentioned above, this module once again returns to a non-functioning state. The most likely cause of this malfunction is a poor solder joint which began to function when either thermal stress (from the temperature change) or mechanical stress (from the instrument swaying) re-established electrical contact.

It is also worth noting that there are significantly more downgoing than east and west-going events. This is expected because the distribution of cosmic-ray arrival directions follows a $\cos \theta$ distribution. The modules are also further apart and present a smaller effective cross sectional area for sideways going events.

The east-west asymmetry, α , can be calculated from the west intensity J_w and the east intensity, J_e , using the formula,

$$\alpha = \frac{J_w - J_e}{0.5 * (J_w + J_e)}$$

Near the geomagnetic latitude of Fort Sumner, NM ($\lambda \sim 41^\circ$), previous measurements at an altitude of 33,000 ft yeilded an asymmetry of $\alpha = 0.055 \pm 0.011$ [10]. Using the data collected during this flight, excluding time periods where the payload was not oriented correctly or malfunctioning, the calculated east-west asymmetry is $\alpha = -0.031$ at float altitude. This result incorrectly claims that more events are arriving from the east than from the west. Given that no corrections were possible for systematic biases in the instrument, this result is not terribly surprising, if somewhat disappointing. It may be possible to use pre-flight data to better estimate the efficiency of the east and west detector arrays and improve this result

While the goal of the project was to measure how the asymmetry changed with altitude, the team has not been able to include HASP GPS altitude data in the analysis at the present time. Given the obvious problems with the asymmetry value mentioned above, it is unclear that such an analysis would provide any scientific insight.

5. Lessons Learned

Although the payload performed reasonably well over the flight, there were several problems that bear mentioning and could have contributed to the inaccurate science result. These have been briefly mentioned previously, but are elaborated upon in more detail below.

Communication outages – There were several times during the flight when the payload stopped transmitting HASP serial data. It is unclear from the data alone whether this transmission outage was caused by the microcontroller locking up or simply ceasing data transmission. The error was fairly easy to correct, only requiring powering the payload off and then back on, but resulted in several hours of missing data (the longest of which was ~2 hours near the end of the payload ascent). This failure mode never presented itself in the lab, even during several overnight data runs. Given the radiation environment at float and the fact that the microcontroller is not rad-hard, it seems reasonable to suspect that radiation may have been part of the cause, but it is impossible to say for sure. Using rad-hard microprocessors may resolve this issue in future flights if other groups have had similar problems and a suitable alternative exists. Closer monitoring of data from the payload during the flight could have significantly reduced the length of the outages.

Rotation problems and e-compass readings – As was mentioned earlier, it is unclear how reliably the e-compass actually determined the heading of due north, potentially due to swaying of the HASP platform. A three-axis e-compass, while requiring more effort to program and interpret data, may have been more accurate during these unforeseen oscillations.

Efforts to rotate the payload to point due south were not successful. While this could have been caught by careful inspection of serial data during the flight and possibly corrected, a far better option would have been to write a subroutine to maintain a southward heading, similar to the one for the northward heading. The code could even be written to switch between facing north and south every half hour or so. This would provide a much better handle on systematic errors, such as one detector orientation having a slightly different aperture than the other. When looking for a small effect with limited statistics, understanding these differences is crucial to getting a reliable result.

SiPM failure – One of the SiPMs was not operational for part of the flight. It is unclear whether this was due to a manufacturing error in the SiPM/amplifier or whether it was a poor electrical connection somewhere within the HARD payload system. The SiPM was never unreliable during lab testing. To minimize the likelihood of such failures in the future, better attention should be paid to quality control and workmanship.

6. Participants

There were six undergraduate students from ECE department advised by two faculty members as shown below. Four students travelled to the CSBF site in July 2013 for the integration and vacuum testing.

Student team members:

Name	Major	Year (as of Fall '13)	Gender	Ethnicity	Race	Disability
Ernest Neiman	Computer Engineering	Undergraduate	Male	non-Hispanic	White	No
Joseph Bennett	Electrical Engineering	Undergraduate	Male	non-Hispanic	White	No
Codi Wasser	Computer Engineering	Undergraduate	Male	non-Hispanic	White	No
Kelvin Joefield	Electrical Engineering	Undergraduate	Male	non-Hispanic	Black	No
Yousef Samkari	Electrical Engineering	Undergraduate	Male	non-Hispanic	Asian – Middle East	No
Abdul Rahman Alzaabi	Electrical Engineering	Undergraduate	Male	non-Hispanic	Asian – Middle East	No

Faculty advisors:

Name	Title	Department	Gender	Ethnicity	Race	Disability
Dr. Wookwon Lee	Associate Professor	Electrical & Computer Engineering	Male	non-Hispanic	Asian	No
Dr. Nicholas Conklin	Assistant Professor	Physics	Male	non-Hispanic	White	No

7. Presentations and Publications

The following presentations and publications have resulted from Gannon University's participation in the HASP program for 2013:

1. E.A. Neiman, III, J. Bennett, C. Wasser, Y. Samkari, K. Joefield, Jr., D. MacKellar, N. Conklin, and W. Lee, "High Altitude Radiation Detector 2 (HARD 2)," presented at the *Fall 2013 Meeting of the Western Pennsylvania Sections of the American Association of Physics Teachers*, October 19, 2013, Erie, PA.
2. W. Lee and N. Conklin, "High Altitude Radiation Detector (HARD): Integration of Undergraduate Research into Senior Design and Lessons Learned," in *Proc. ASEE Annual Conference and Exposition*, June 23-26, 2013, Atlanta, GA.
3. E.A. Neiman, III, J. Bennett, C. Wasser, Y. Samkari, K. Joefield, Jr., N. Conklin, W. Lee, and D. MacKellar, "High Altitude Radiation Detector," a poster presentation at the *Celebrate Gannon – Undergraduate Research*, April 10, 2013, Erie, PA.

8. Reflections and Implications

As mentioned previously, six undergraduate students from the ECE department, including one current senior and five juniors (as of Fall 2013), participated in the project. One of the five juniors was involved in the design of HARD PL02 in 2012 and continued his involvement in 2013 for HARD PL03. Four other current juniors and one current senior joined the team in the beginning of Spring 2012. The student team met regularly for about 5 hours of lab work per week during the spring and fall semesters of 2013.

This project provided a great framework for undergraduate students in research and greatly enhanced their learning experience outside of class. One of the challenges in carrying out the overall project activities was time management amid team member's schedules. Student team members normally carry 15~18 credit hours of coursework each semester, as well as additional extracurricular activities. Weekly meetings were crucial for ensuring successful completion of the project by a set-deadline. The project was very helpful in teaching team members the concept of delivering a product on schedule, which is an essential workplace skill that cannot be taught in a class. It also facilitated close collaboration between students and faculty.

Students' travel to an off-campus site for intercollegiate collaboration, i.e., integration of the payload onto the HASP instrument at the CSBF site, was a great way to enhance their overall learning experience and enthusiasm for this project.

9. Concluding Remarks

Built on the lessons learned from the previous year's payload, the payload HARD-PL03 was a success and was able to collect the desired cosmic-ray data, albeit without measuring an asymmetry value that is

consistent with the accepted result that cosmic-rays are predominantly positively charged. All other parts of the design, including serial communications, payload orientation, and temperature monitoring, functioned as expected.

Additionally, this project provided student team members with an excellent engineering opportunity that requires both technical and non-technical skills to solve real-world problems. This project has effectively facilitated building a solid basis of technical expertise at Gannon University, particularly in electrical and computer engineering and physics, and is creating opportunities to engage undergraduate students in other research projects. In particular, with the experience that the students acquired from HARD-PL02 (in 2012) and PL03 (in 2013), the Gannon team is currently developing a payload for NASA's Undergraduate Student Instrument Project (USIP) that is expected to take 18 months for completion and use a commercial ballooning carrier. Due to the increased complexity and extended timeline of the project, Gannon's USIP project cannot use HASP 2014 as a carrier, although HASP would be an ideal platform for such a payload. As such, Gannon will skip applying for HASP 2014, but plans to put forward an application in 2015 or beyond, perhaps flying a refurbished version of the USIP payload.

HASP has been an invaluable tool to prepare our students for leadership roles in research and the workplace. We give the program our most enthusiastic endorsement and hope it continues for many years to come.

References

- [1] Gannon University HARD project team, "High Altitude Radiation Detector (GU-HARD-PL03)," *HASP 2013 proposal submitted to the HASP 2013 Program*, 12/14/2012.
- [2] Photoniques SA, *1.3mm² active area, low noise solid state photomultiplier for visible and near-IR light applications*, Data sheet, Doc. No.: SSPM_0905V13MM, Sept. 2009.
- [3] Application circuit diagram for AMP-0604 and AMP-0611, Photoniques SA, available on line at http://www.photonique.ch/Prod_AMP_0600.html.
- [4] Honeywell, *Digital Compass Solution HMC6352*, data sheet, available on line at <https://www.sparkfun.com/products/7915>.
- [5] Analog Devices, *AD8615/AD8616/AD8618: Precision, 20 MHz, CMOS, Rail-to-Rail Input/Output Operational Amplifiers*, data sheet, 2008.
- [6] Digilent, *chipKIT™ Uno32™ Board Reference Manual*, Doc: 502-209, October 25, 2011.
- [7] Maxim Integrated Products, Inc., *+5V-Powered, Multichannel RS-232 Drivers/Receivers*, 2006, datasheet 19-4323; Rev 15; 1/06, available at <http://pdf1.alldatasheet.com/datasheet-pdf/view/73050/MAXIM/MAX233.html>.
- [8] Murata NDY2405C, *NDY Series: Isolated 3W Wide Input DC/DC Converters*, data sheet, Doc. No.: KDC_NDY.F02, 2012.
- [9] Recom Power, RS-2415DZ, *ECONOLINE DC/DC-Converter*, REV: 0/2012.
- [10] W. C. Barber, "East-West Asymmetry and Latitude Effect of Cosmic Rays at Altitudes up to 33,000 Feet," *Physical Review*, pp. 590-599, 1949.

Appendix

A-1. Software Subroutines for Micro-processor

The following programming codes were implemented in Arduino for the necessary functionality:

- FlightCode.pde: Main program to integrate all subroutines and download the codes onto the microcontroller
- M01_GPS.pde: for GPS-related functions
 - void SetupGPS()
 - void GetOnboardGPSString()
 - void GetGPSTime(char *str, unsigned int size, char *time)
 - void ParseGPSString(unsigned char *str, unsigned int size)
- M02_RadDet.pde: for radiation detection-related functions
 - void SetupRadDet()
 - int GetHit()
- M03_SDmemory.pde: for memory card-related functions
 - void SetupSD()
 - int GetFilename()
 - void WriteEvent()
 - void Reboot()
- M04_Servo.pde: for control of a servo motor
 - void SetupServo()
 - void PointNorth()
 - int ControlServo(float heading)
 - void ServoRotate(Servo *s, float angle)
 - inline float MicrosecondsToAngle(float micro)
 - inline float CheckAngle(float angle)
- M05_eCompass.pde: for electronic compass-related functions
 - void SetupECompass()
 - float GetHeading()
 - void CalibrateCompass()
- M06_HASPSerial.pde: for serial communication-related functions
 - void ReadHASPSerial()
 - void SendHASPSerial()
- M07_TempSensor.pde: for temperature sensor-related functions
 - float GetTemp()